The International Journal of Advanced Manufacturing Technology (2019) 103:2761–2772
https://doi.org/10.1007/s00170-019-03534-3

ORIGINAL ARTICLE

NiMn-based Heusler magnetic shape memory alloys: a review

T. Bachaga [1,2,3] · J. Zhang [1] · M. Khitouni [2] · J. J. Sunol [3]

Received: 14 November 2018 / Accepted: 27 February 2019 / Published online: 27 April 2019

Abstract
The use of magnetic shape memory alloys ($MSMA_s$) in manufacturing industry has increased significantly in recent years. This is mainly due to their great interest in their potential applications in smart devices, because of the reversible distortions suffered. The well-known example of these combinations is the Heusler type. A review is given of experimental works concerning the examination of magnetic field, structural phase transitions, and the magnetocaloric impact in Heusler Ni–Mn–X (X = In, Sn, Sb) and Ni–Co–Mn–Y (Y = In, Sn, Sb) alloys. This type of compounds has excellent properties, for example, the presence of coupled magnetostructural (coïncident magnetic and martensitic transitions) and metamagnetostructural phase transitions (coïncident metamagnetic (ferromagnetic-antiferromagnetic) and martensitic transitions), the magnetocaloric impact (MC), and the large magnetoresistance change (MR). The conceivable difficulties and remaining problems are briefly discussed.

Keywords Heusler alloys · Martensitic transformation · Magnetic shape memory alloys · Magnetocaloric · Metamagnetic alloy

1 Introduction

In previous decades, Heusler-type magnetic shape memory alloys ($MSMA_s$) have an increasing interest in technological applications, because of their excellent properties. These multifunctional properties include magnetic transformation [1], reversible distortion [2, 3], giant magnetoresistance (MR) [4], and extensive magnetocaloric effect (MCE) [5, 6]. These properties make them especially interesting for the creation of new magnetic sensors, actuators, and magnetic coolant for magnetic refrigeration [7–9]. The main cause of the distortion of the structure is the martensitic transformation experimented by these materials from a high-temperature ordered cubic austenite phase to a low-temperature tetragonal, orthorhombic, or monoclinic disordered martensite phase. The structural change is displacive and diffusion less. At that point, the ferromagnetic-paramagnetic transition is experienced when the Curie limit is exceeded. This structural and magnetic progress can be created by two causes: magnetic field application or temperature change. Based on diffusion less phase transformation, which is called martensitic transformation, the shape memory effect (SME) in alloys is known to be novel conduct by which a deformed alloy in the low-temperature phase recuperates its original shape by reverse transformation upon heating to the reverse transformation temperature. This impact was observed for the first time in Au–Cd alloys in 1951 and turned out to be notable with its disclosure in Ti–Ni compounds in 1963 [10, 11]. The Ti–Ni alloys are the most recognizable shape memory alloys (SMA_s), with applications in different fields, such as cellar-phone antennae, medical guide wires, and smart actuators. Since the strain and stress created by the SME are extremely large as compared to those created in magnetostrictive and piezoelectric materials, SMA_s are potential candidates for actuators, for example, motors and supersonic oscillators. Be that as it may, since the output actuation in SMA_s happens through temperature change for an input signal, it is difficult to get a fast response to the input signal at frequencies high than 5 Hz, because the thermal conductivity of the alloys is a rate determining factor of the response [12]. This fatal drawback limits the use of SMA_s as actuators. $MSMA_s$ in which a rapid output strain is obtained by the application of a magnetic field have been produced to overcome this obstacle.

✉ T. Bachaga
bachagatarak@yahoo.fr

J. Zhang
zhangjh_radicas@163.com

[1] School of Computer Sciences and Technology, University of Qingdao, Qingdao, China

[2] Laboratory of Inorganic chemistry, UR-11-ES-73, University of Sfax, 3000 Sfax, Tunisia

[3] Dep. de Fisica, Universitat de Girona, Campus Montilivi, 17071 Girona, Spain

The most considered $MSMA_s$ are those called Heusler alloys. These mixtures are a well-known sort of association of intermetallic mixtures containing more than 1500 members, discovered by Fritz Heusler in 1903. He has analyzed a combination of Cu, Mn, and Al is ferromagnetic, although this is not the case for all three fundamental components [13, 14]. The reason for this originates from the special crystallographic structure of the material. The Cu_2MnAl was the principle Heusler compound. This combination exhibited an austenitic phase at room temperature whose structure was totally chosen 3 decades later by Bradley and Rodgers [15]. They demonstrated a cubic structure $L2_1$ with the space group $Fm\bar{3}$ m and a lattice parameter a = 5.949 Å and a unit cell composed of eight atoms of Cu and four atoms of Mn and Al. These alloys are ternary semiconductor or metallic materials. The last has two stoichiometries, one of type 1: 1: 1 (half-Heusler alloys) and the other of type 2: 1: 1 (full-Heusler alloys) [16]. These days, they possess a hot area of research [17]. The general stoichiometric formula of full-Heusler alloys is X_2YZ. The crystal structure is illustrated in Fig. 1. The X, Y, and Z components include four distinctive fcc (face centered cubic) lattices, which are moved along the spatial diagonal. It is referred to as the $L2_1$ Heusler structure with the space group $Fm\bar{3}$ m. The atoms X are arranged on the (0, 0, 0) and the (½, ½, ½) lattice, whereas, the Y and Z atoms occupy the (¼, ¼, ¼) and the (¾, ¾, ¾) lattices, respectively [17]. There is another structure B2, appeared in Fig. 1, for the disordered state. In this case, the Y and the Z lattices are mixed. Thus, the unit cell can be described as a bcc (body centered cubic) lattice with X atoms in the corners and Y and Z atoms with half inhabitance in the center position [17]. The class of magnetic mixtures X_2YZ and XYZ has multifunctional magnetic properties, for example, magnetooptical, semi-metallic ferromagnetic element, magnetooptical effect, shape memory effect, topological covers, and magnetocaloric and magnetostructural characteristics [18–22]. For the most part, these combinations were mass polycrystalline obtained by arc melting, followed by a high-temperature annealing, or single crystals created by the Czochralski technique [23–25]. Indeed, the fast quenching by melt-spinning offers three potential focal points for making practical devices: the shape of the ribbon, the avoidance of the annealing allows a better homogenization of the phase, and the fact that it's easy to obtain highly textured ribbons. Among the melt-spinning conditions can be mentioned the pressure of the ejection gas, the device geometry, the melting temperature, the clearance between a nozzle and the wheel surface, and the rotational speed of the wheel that influences the structure of the ribbon and their dimensions [26]. The crystallization energy occurs during the change of these parameters and the heat exchange. The melt-spinning has been completed out in several shape memory systems: Mn–Ni–Sn, Ni–Mn–In–Co, and Fe–Pd [26–28]. One of the essential cases detailed in a Heusler type combination dates back to 1999 [29].

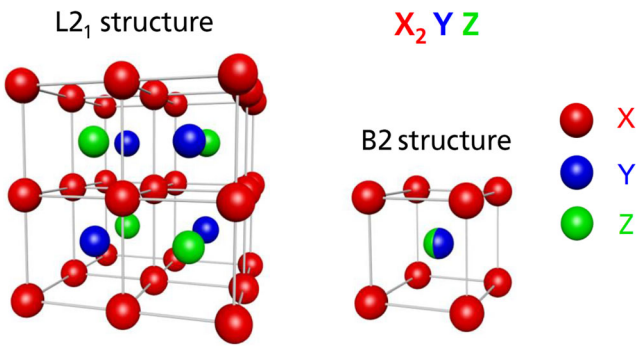

Fig. 1 Schematic illustration of the $L2_1$ and the B2 structure of a Heusler alloys with the chemical composition X_2YZ. The X, Y, and Z atoms, which are shown in red, blue, and green respectively, occupy different sublattices. Reproduced from reference [17]

Throughout the years, martensitic transformations (MT) have not been found in full-Heusler alloys, with the exception of Ni_2MnGa that experiences an MT and no volume change occurs over the progress [30–33]. These days, the martensitic transformation is uncovered at appropriate off-stoichiometric structures for any of the Ni_2MnZ combinations (with Z = Ga, Sn, In, Sb) [34, 35]. The distinctions are that in these mixtures, in contrast with stoichiometric one, a volume change occurs during the martensitic progress, depending on the Z species [36] (see Fig. 2). The Heusler Ni–Mn–Ga combinations are the most considered alloys [37]. They demonstrate the interesting fact that they are the main ones exhibiting magnetic properties in their stoichiometric composition, whereas, other Heusler magnetic alloys show these properties only in off-stoichiometry. However, in order to overcome the generally low martensitic transformation temperature in the range between 180 and 200 K and the high cost of Ga, the search for alloys free Ga has recently attempted, specifically by displaying distinctive components, for example, In, Sn, or Sb. Krenke et al. [38, 39] inquired without Ga-free Heusler $MSMA_s$ supplanting Ga with Sn and In. They revealed a full standard examination of Ni–Mn–Sn [38] and Ni–Mn–In [39].

This article is restricted to NiMn-based Heusler magnetic shape memory alloys since it will be hard to consolidate the information from a broad number of productions on an extent of ferromagnetic compound systems, the vast majority of which just flag another piece with an enhanced magnetostructural characteristic. The principal fragment of this paper analyzes the impact of structural variation on the magnetic, and mechanical properties of various Heusler Ni–Mn–X (X = In, Sn, Sb) combinations. The second fragment of this paper deals with the connection among structure and properties of Ni–Co–Mn–Y (Y = In, Sn, Sb) systems. The structure-property correlation and furthermore the remarkable properties of Heusler combinations are investigated in various possible applications.

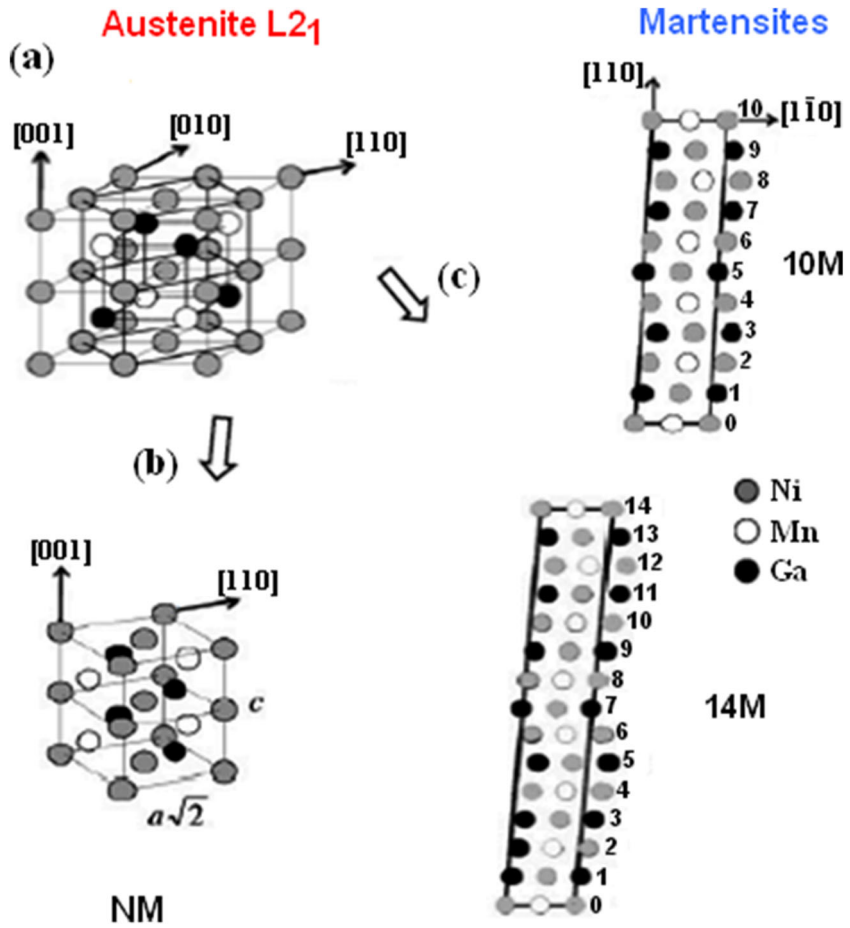

Fig. 2 Crystal structure of the $Ni_{50}Mn_{50-x}Z_x$ (Z = In, Sn and Sb) alloys: (a) structural transition from the phase with a cubic lattice of the $L2_1$ type into a phase with a tetragonal structure of the $L1_0$ type; (b) and (c) lattice distortions in the 10 M and 14 M phases, respectively. Reproduced from reference [36]

2 Characteristics and properties of Heusler Ni–Mn–X (X = In, Sn, Sb) alloys

Recent research concerning the new $MSMA_s$ of the Ni–Mn–X (X = In, Sn, Sb) alloys appears instead of the Ni–Mn–Ga alloy. This is due to the presence of a coupled magnetostructural transition in non-stoichiometric compositions. The magnetostructural change of these new Heusler alloys is joined by an inverse magnetocaloric effect and giant magnetoresistance [5, 6, 36, 40, 41].

2.1 Structure and phase change of Heusler Ni–Mn–X (X = In, Sn, Sb) alloys

The magnetostructural transitions are shown in the Ni–Mn–X (X = In, Sn, Sb) alloys, which are joined by a magnetocaloric effect and giant magnetoresistance [41–57]. Takenaga et al. [41] exhibited that $Ni_2Mn_{2-x}Sn_x$ alloys near to stoichiometry (x = 0.3) have a cubic structure of type Heusler $L2_1$ with a parameter of 6 Å. They have demonstrated that a slight increase in the level of Mn atoms in these alloys leads to the presence of a basic progress austenite-martensite during a temperature change. Hernando et al. [42] studied the magnetostructural development of Heusler NiMnSn and NiMnIn alloys. They showed that the alloys are monophase and that ferromagnetic $L2_1$ austenite is a high-temperature parent phase. In addition, at a low temperature, the austenite is converted into a martensite with a system-dependent symmetry modulated structure (orthorhombic 7 M, monoclinic 10 M, and monoclinic 14 M). Krenke et al. [37] studied the structural change in $Ni_{0.5}Mn_{0.5-x}Sn_x$ alloys. They have shown that the structure of martensite is of the 10 M, 14 M, or $L1_0$ type, whereas, that of austenite is of the $L2_1$ type, on the basis of the Sn composition. In addition, they are showing that both phases are ferromagnetic in $Ni_{0.5}Mn_{0.5-x}Sn_x$ alloys. For the Heusler $Ni_{0.5}Mn_{0.5-x}In_x$ alloys, they experience martensitic transformations in the scope of $0.05 \le x \le 0.16$, while, in the $0.16 \le x \le 0.25$ range, the alloys retain the cubic stage. At the point when x = 0.16, the magnetic field-induced structure transformation (MIST) occurs, and martensitic change moves 42 K in the 5 T field [38]. The structural change in Heusler $Mn_{50}Ni_{50-x}(Sn, In)_x$ alloys is studied in references [43–45]. These studies have shown that the martensitic transformation (from austenite with cubic $L2_1$ structure to martensitic phase with 14 M modulated monoclinic structure) was detected in $Mn_{50}Ni_{50-x}Sn_x$ and $Mn_{50}Ni_{50-x}In_x$ samples. Yiwen et al. [49] studied the structural change in $Mn_{50}Ni_{50-x}Sn_x$ (x = 7–10) alloys. The martensite phase is recognized to be modulated

monoclinic 6 M; however, the austenite is with $L2_1$ cubic structure. At the moment when the Sn content is 7–9%, there is no obvious magnetization difference related to martensitic transformation, since the martensitic transition happens from a paramagnetic austenite to powerless magnetic martensite. For the ribbons with Sn content of 10%, the martensitic transformation occurs from ferromagnetic austenite to brittle magnetic martensite. Khan el al. [50] have demonstrated that Heusler $Ni_{50}Mn_{25+x}Sb_{25-x}$ alloys have a martensitic phase transitions above than 150 K, with $7 < x \leq 10$. The martensitic stages are of orthorhombic structure (space group, Pmm2) in alloys with $13 \leq x \leq 14$, whereas, the austenitic phases show a cubic structure $L2_1$ in alloys with $0 \leq x \leq 12.5$. When the concentration of Mn increases, the martensitic transformation increases rapidly, though, the Curie temperatures of the austenitic stages decrease straightly with the expansion of x.

Which of such structures stabilize in the martensitic transformation of the Ni–Mn–X alloys depends on the composition. The phase diagrams of Ni–Mn–based Heusler alloys are shown in Fig. 3. In these phase diagrams, the magnetic and martensitic phase change temperatures are plotted as a function of the valence electron concentration per atom (e/a) for Ni–Mn–Ga, $Ni_{50}Mn_{50-x}In_x$, $Ni_{50}Mn_{50-x}Sn_x$, and $Ni_{50}Mn_{50-x}Sb_x$ alloys [33]. It very well may be seen that the structure changed from cubic→10 M→14 M→$L1_0$ with an increasing (*e/a*) and temperature, in Fig. 3(a–c). But in Fig. 3(d), the alloy follows the next sequence cubic→ 4 O–sevenfold (mixture)→ $L1_0$. The 4 O modulated structure is also observed, for the Sn alloy [33].

The correlation analysis between the width of the composition zones and species X, in the phase diagrams, describes the structural and magnetic changes. It's also noted that the crystalline structure of martensite depends on the conditions of elaboration. For example, Santos et al. [51] observed a 7 O orthorhombic martensite in a $Ni_{50}Mn_{37}Sn_{13}$ alloy with melt spinning technique; while, Muthu et al. [52] found an 4 O orthorhombic martensite, in $Ni_{50}Mn_{37}Sn_{13}$ alloy obtained with arc melting technique. Hernando et al. [42] reported that the orthorhombic structure is 10 M modulated for $Ni_{50}Mn_{37}Sn_{13}$ ingots and is a 14 M orthorhombic martensite modulated for $Ni_{50}Mn_{37}Sn_{13}$ ribbons.

2.2 Properties of Heusler Ni–Mn–X (X = In, Sn, Sb) alloys

The understanding of the possible appearance of the magnetostructure transition and inverse MCE is essential to study presence of the magnetic exchange interaction between the martensitic and austenitic phases in these alloys resulting in the presence of magnetization jumps. Krenke et al. [53] studied for the first time the inverse MCE in alloys: $Ni_{50}Mn_{35}Sn_{15}$ and $Ni_{50}Mn_{37}Sn_{13}$. The measurements ΔS_M were performed and based on the Maxwell relation. The maximum variation of the entropy is equal to ~ 15 J kg^{-1} K^{-1} at T_m = 185 K for the $Ni_{50}Mn_{35}Sn_{15}$ alloy and for the $Ni_{50}Mn_{37}Sn_{13}$ alloy was ~ 20 J kg^{-1} K^{-1} at T_m = 305 K, upon the change in the magnetic field ΔH = 5 T. The magnetostructural behavior and the magnetocaloric properties of the $Mn_{50.5-x}Ni_{41}Sn_{8.5+x}$ alloys with (x = 0, 1, and 2) were studied by Ghosh et al. [54]. They showed that the entropy change ~ 11.85 J kg^{-1} K^{-1} was obtained for x = 0 at 270 K under a magnetic field of 1.5 T. They demonstrated that the net refrigerant capacity was evaluated at − 44.82 J kg^{-1} for a similar example, which turned out to be larger than that of other Ni–Mn–Sn alloys. This causes the obtaining of a magnetoresistance of about 33% for these alloys within the sight of 8 T attractive field contrasts. Caballero-Flores et al. [55] considered the thermomagnetic properties and magnetocaloric effect in Heusler $Ni_{50.3}Mn_{36.5}Sn_{13.2}$ alloy ribbons. They showed that the maximum value of entropy about ~ 17.3 J K^{-1} kg^{-1} for an applied magnetic field of 3 T. The inverse magnetocaloric impact of bulk $Ni_{2+x}Mn_{1.4-x}Sn_{0.6}$ (x = 0, 0.06, 0.12, 0.18) Heusler alloys is researched by Ray et al. [56] (see Fig. 4). They demonstrated that the change in magnetic entropy at first extended with abundance Ni focuses up to x = 0.12 in any case, then a drastic fall in value is observed for the sample x = 0.18, but, the relative cooling power (RCP) value is increased continuously with the excess Ni concentration. The effect of Sn content on mechanical, magnetization, and shape memory behavior in NiMnSn alloy is researched by Aydogdu et al. [57]. It was revealed that the $Ni_{50}Mn_{40}Sn_{10}$ alloy have a good shape memory effect with 2.1% recoverable strain and completely reversible superelasticity at high temperatures (190 °C). The

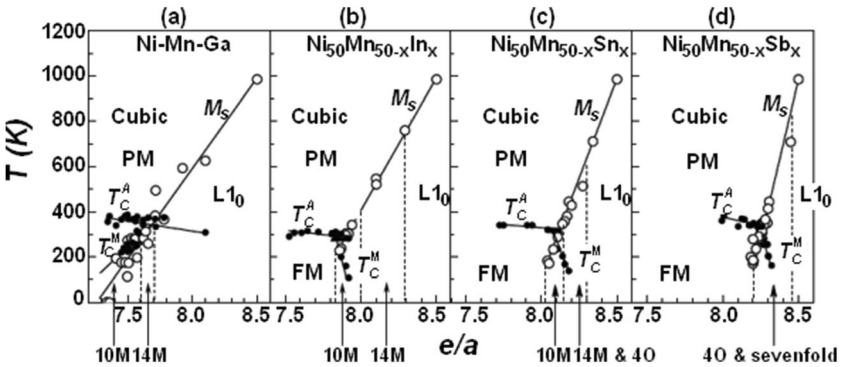

Fig. 3 The magnetic and structural phase diagram of Heusler Ni–Mn–X alloys with X as **a** Ga, **b** In, **c** Sn, and **d** Sb. The regions corresponding to the different structures are separated by dashed lines. Reproduced from reference [33]

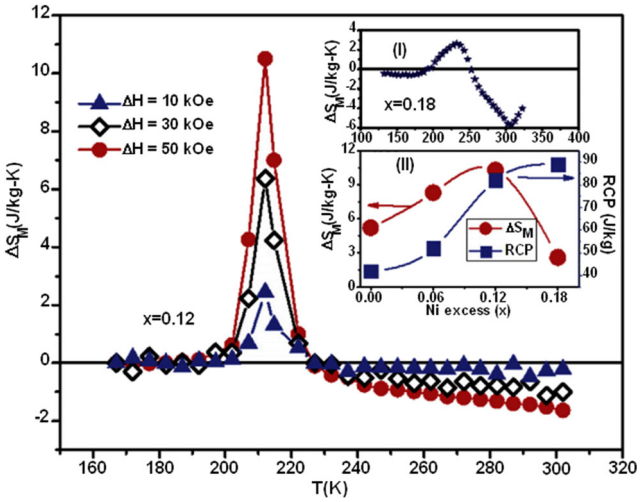

Fig. 4 Temperature variation of ΔS_M for $x = 0.12$ sample and (I) is showing variation of ΔS_M for $x = 0.18$ sample and (II) variation of ΔS_M and RCP value with the excess Ni concentration. Reproduced from reference [56]

$Ni_{50}Mn_{39}Sn_{11}$alloy failed at 650 MPa and 7% during compressive deformation. Tan et al. [58] studied impacts of fractional substitution of Fe element for Ni element in the structure, martensitic transformation, and mechanical properties of NiFeMnSn alloys. They demonstrated that the mechanical properties of Ni–Mn–Sn alloy can be essentially improved by Fe addition. The $Ni_{47}Fe_3Mn_{38}Sn_{12}$ alloy has accomplished a maximum compressive strength of 855 MPa with a fracture strain of 11%.

Stern-Taulats et al. [59] studied the magnetic caloric effect in a low-hysteresis $Ni_{51}Mn_{33.4}In_{15.6}$ metamagnetic shape memory (see Fig. 5). They noted that the maximum variation of entropy in the martensitic transition region (T_m = 304 K) under the variation of the magnetic field equal to 5 T is ΔS_m = 15 J kg^{-1} K^{-1}. Thus, that the magnetocaloric effect is inverse, which is consistent with the fact that the transition temperatures pass to lower values under an applied magnetic field. Rosa et al. [60] showed the annealing influence on the martensitic transition and the magnetic entropy change in a $Ni_{45.5}Mn_{43.0}In_{11.5}$ shape memory alloy. They showed that the annealing at 873 K was the best choice for high entropy variation; however, the other annealing at 973 and 1073 K. The giant elastocaloric impact of directionally solidified Ni–Mn–In magnetic shape memory alloys is researched by Huang et al. [61]. It was uncovered that the $Ni_{48}Mn_{35}In_{17}$ alloy has a good reversibility of the giant elastocaloric with 1.4% recoverable strain. These adiabatic stress-strain curves present fully recoverable superelasticity of about 1.1% transformation strain.

Khan et al. [62] reported the inverse magnetocaloric effect in ferromagnetic $Ni_{50}Mn_{37+x}Sb_{13-x}$ Heusler alloys and observed the best extent of the inverse MCE. The maximum estimation of ΔS_m is 20 J kg^{-1} K^{-1} in $Ni_{50}Mn_{38}Sb_{12}$ at 297 K for a magnetic field change of 5 T as compared to the concentrations $x = 0.5$ (ΔS_m (T_m = 284 K) = 15.0 J kg^{-1} K^{-1}) and $x = 0$ (ΔS_m (T_m = 273 K) = 18.2 J kg^{-1} K^{-1}). The exploratory investigations of magnetocaloric effect in $Ni_{50-x}Mn_{38+x}Sb_{12}$ alloys with $x = -1$, 0, 1, and 2 performed by Feng et al. [63] (see Fig. 6). An extensive reversible negative above room temperature was founded. The most extreme estimation of ΔS_m is 5.21 J kg^{-1} K^{-1} in $Ni_{49}Mn_{39}Sb_{12}$ at 347 K for a magnetic field change of 5 T.

The mixture Co with Ni–Mn–X (X = In, Sn, Sb) alloys has a significant influence on the magnetic and mechanical properties, more precisely on the behavior of the magnetization. The Cobalt concentration also greatly affects the magnetic properties of these alloys.

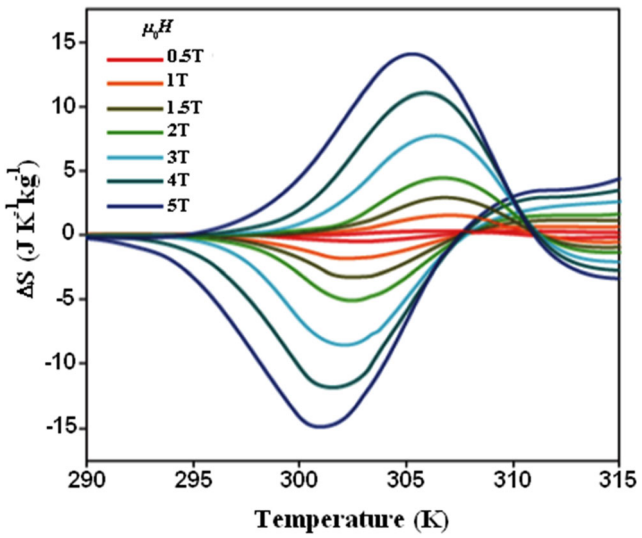

Fig. 5 Field-induced entropy changes at selected values of the applied/removed magnetic field from magnetization measurements. Reproduced from reference [59]

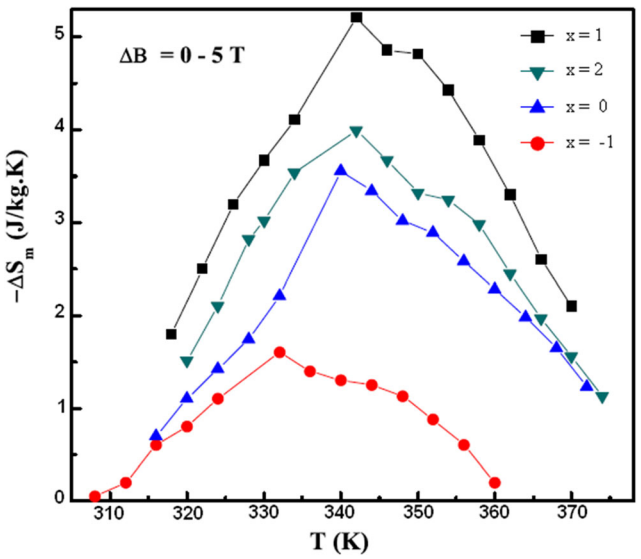

Fig. 6 Temperature dependences of the magnetic entropy change in the $Ni_{50-x}Mn_{38+x}Sb_{12}$ alloys with $x = -1$, 0, 1, and 2, respectively, for a magnetic-field change from 0 to 5 T. Reproduced from reference [63]

3 Characteristics and properties of Heusler Ni–Co–Mn–Y (Y = In, Sn, Sb) alloys

In Heusler Ni–Mn–X alloys, the attractive coupling between the closest Mn particles is probably to be antiferromagnetic. However, by doping Co to supplant a piece of the Ni particles, the attractive coupling of Mn–Mn must be initiated for to be ferromagnetic. In this way, the expansion of Co for Ni builds the Curie point, the magnetic moment of the austenitic stage, and the magnetization at the MT. A remarkable behavior of the Ni–Co–Mn–Y alloys is the possibility of inciting the opposite transformation by an attractive field and the related metamagnetic shape memory impact, i.e., the recuperation of a past strain by means of field-initiated inverse MT.

3.1 Characteristics and properties of Ni–Co–Mn–In alloys

Recent studies demonstrate that the substitution of Nickel by Cobalt in Heusler Ni–Mn–In alloys firmly influences magnetocaloric and magnetic properties. Besides, Co-doping will not only improve magnetization of the magnetic phase of Ni–Mn–In, yet additionally enhance fundamentally upgrade metamagnetic properties, including the metamagnetic shape memory impact and the magnetocaloric effect. The Ni–Co–Mn–In alloys have numerous favorable advantages of the application, for example, the composition does not contain rare earths or harmful components, super-elastic deformation, great protection from oxidation, simple make, high machining, and high adiabatic temperature change at low field [64]. Huang et al. [65] detailed that the extensive reversible MCE in a $Ni_{49.8}Co_{1.2}Mn_{33.5}In_{15.5}$ magnetic shape memory alloy was acquired with a 7 M monoclinic structure. They demonstrated that the extensive reversible magnetic entropy change of 14.6 J kg^{-1} K^{-1} and a wide operating temperature window of 18 K under 5 T were all the while accomplished, connected with the low thermal hysteresis (8 K) and large magnetic-field-induced move of change temperatures (4.9 K T^{-1}) that prompt to a narrow attractive hysteresis (1.1 T) and little normal magnetic hysteresis loss (48.4 J kg^{-1} under 5 T) as well. This difference in parameters is critical for enhancing the magnetocaloric performance.

The impact of the atomic order on the martensitic transformation entropy change has studied in a Ni–Mn–In–Co metamagnetic shape memory alloy by Monroe et al. [66]. It is affirmed that the entropy change advances as a result of the variations on the degree of $L2_1$ atomic order brought by thermal treatments, although, in opposition to what happens in ternary Ni–Mn–In. The entropy change value between around 40 and 5 J^{-1} kg^{-1} K^{-1} can be acquired in a controllable for a single alloy under the fitting maturing process, which drawing out the possibility of appropriating tune the magnetocaloric effect. For the Heusler $Ni_{45}Co_5Mn_{37}In_{13}$ alloy at 1 T [67], when martensitic transition happened, the most extreme difference in magnetization $\Delta M = 90$ A m^2 Kg^{-1} was gotten. The martensitic structure is 6 M structure modulated with a = 0.4393 nm, b = 0.5572 nm, c = 1.296 nm, and $\beta = 93.83°$.

Kainuma et al. [2] examined the attractive field-actuated shape recuperation by reverse phase transformation of $Ni_{45}Co_5Mn_{36.6}In_{13.4}$ alloy. The structure has cubic $L2_1$ structure with a = 0.5978 nm, and the Curie temperature is T_C = 382 K. After cooling, a martensite stage change happens at a particular martensitic transformation temperature around room temperature, joined by large magnetization change (ΔM). Li et al. [68] revealed that the vast reversible MCE in a $Ni_{45.3}Co_{5.1}Mn_{36.1}In_{13.5}$ alloy was obtained with an austenite $L2_1$ cubic structure. Furthermore, a substantial reversible ΔS_M above room temperature was observed. The most extreme estimation of ΔS_M is 16.7 J kg^{-1} K^{-1} for a magnetic field change of 5 T.

As of late, the mechanocaloric impact (including barocaloric effect and elastocaloric effect) and magnetocaloric effect in Heusler Ni–Co–Mn–In alloys have progressively pulling in consideration [69–71]. Liu et al. [5] revealed the inverse MCE amid the attractive field-initiated strains in $Ni_{45.2}Co_{5.1}Mn_{36.7}In_{13}$ alloy. They mentioned the temperature change is imperative to such an extent that $\Delta T_{ad} = -6.2$ K at 317 K in ΔH = 1.9 due to large reverse MCE. Although, the giant ΔT_{ad} is getting just in the main stacking of field, but it strongly decreases after the cycle runs out of the field. Among the elements that reason the decrease of ΔT_{ad}, the hysteresis is the fundamental factor in this first-arrange progress. The irreversible energy loss caused by hysteresis altogether decreases the efficiency in magnetic refrigeration applications.

In Heusler $Ni_{49.26}Mn_{36.08}In_{14.66}$ combination, an external pressure displaces the martensitic change temperature T_t by 2 $K.kbar^{-1}$ [72], while, for the $Ni_{45.2}Mn_{36.7}In_{13}Co_{5.1}$ alloy, this expansion of T_t is 4.4 K $kbar^{-1}$, which is considerably more articulated. It's in this manner additionally critical to show that converse MCE materials, for example, Ni–Mn–Co–In exhibit an ordinary barocaloric impact. The magnetic hysteresis is illustrated in Fig. 7. It can be impressively decreased if the sample is charged without bias stress but demagnetized under an external hydrostatic pressure of 1.3 kbar. Moreover, the theoretical calculations give that the efficiency of a magnetocaloric material can be improved by all the while and precisely changing the magnetic field and the pressure, with respect to an apparatus in which just the magnetic field can be adjusted [73].

In Ni–Co–Mn–In system, a relatively flawless shape recuperation strain of about 3% can be acknowledged by applying both steady and single pulsed magnetic fields of 7 T [74]. This sort of shape memory alloy is known a metamagnetic shape memory alloy since it is caused by a metamagnetic change.

Feng et al. [75] examined the improvement of mechanical property and large shape recuperation of sintered Heusler

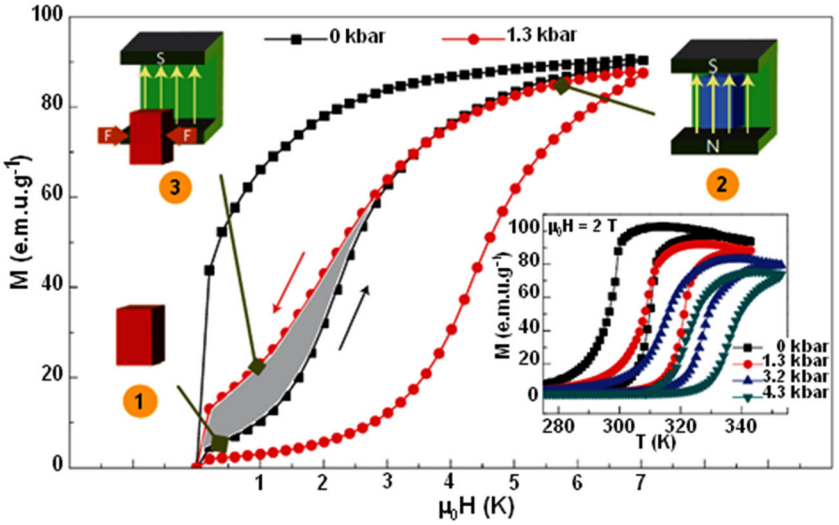

Fig. 7 The large thermal irreversibility can be overcome by the combination of applied magnetics and mechanical forces. M–T curves under 0 and 1.3 kbar hydrostatic pressure at 308 K are shown for $Ni_{45.2}Mn_{36.7}In_{13}Co_{5.1}$. The forward and reverse transitions can be induced in a relatively low field (with little hysteresis-shaded region in the main figure) when the sample is magnetized in zero pressure but demagnetized under an external pressure. Reproduced from reference [74]

$Ni_{45}Mn_{36.6}In_{13.4}Co_5$ alloy. The mechanical properties of $Ni_{45}Mn_{36.6}In_{13.4}Co_5$ bulk sintered at 873 K with 60 MPa compressive stress are improved comparing with the as-cast ingot with same nominal composition. The strain and compressive fracture strength of it are 14% and 1200 MPa, respectively. While, the strain and compressive fracture strength of bulk sintered at 1073 K with 40 MPa are 9.5% and 800 MPa, respectively. The presence of texture benefits the strength and plasticity of it. The recoverable strain is 11.4% and 7.0% for the sample sintered at 873 K with α fiber texture ([100]//ND) under different compressive pre-strain and 7.8% for sample sintered at 1073 K without obvious texture, while, the recoverable strain is only 5.3% for the as-cast ingot with same pre-strain. All the recoverable strain of sintered sample is larger than 90%, while, that of the as-cast ingot is only 66.7%. This demonstrates that the improvement of mechanical property and texture both have effect on the expansion of recoverable strain.

3.2 Characteristics and properties of Ni–Co–Mn–Sn alloys

The Ni–Co–Mn–Sn system is another $MSMA_s$ system pursued by the Ni–Co–Mn–In system. The Ni–Co–Mn–Sn system is a phenomenal possibility for a magnetic shape memory alloy for practical applications since it contains no costly segments and magnetic elements can be acquired. Also, good mechanical properties play an important role in the practical application of Ni–Mn–Sn $MSMA_s$. To completely comprehend the multifunctional properties of these alloys, it is very important to study in detail their magnetic and mechanical properties and their basic changes. Nevertheless, despite several examinations that have concentrated principally because of Co-addition on the magnetocaloric impact [76, 77], there have been a couple of methodical and definite investigations of composition-dependent magnetobasic change in this system.

Deltell et al. [78] considered the structural and thermal behavior of melt-spun alloys of the Ni–Mn–Sn–Co system. They indicated that the martensitic structure comprised of 4 O orthorhombic in samples with a higher (Mn/Sn) proportion and 14 M monolayers with 7 modulated layers in samples with a lower (Mn/Sn) proportion. Also, a change in the martensitic crystalline structure of 14 M to 4 O occurs with the decrease of the martensitic transition temperature. They suggested that the internal pressure be incited by the firmly situated microstructure, which prompts to the decrease of the progress temperature due to a refined martensite plate and to the formation of thick martensitic variants of different orientation. In addition, it has also been found that the partial substitution of Ni by Co shifts martensitic change to bring down to lower temperatures in Ni–Mn–Sn–Co compounds [77].

For compositional improvement purposes behind $MSME_s$, a recent investigation of the phase diagram of the Ni–Co–Mn–Sn alloy in the high-temperature range has established [79]. Be that as it may, the phase diagram in the low temperature extend has never been investigated. The foundation of the complete phase diagram of the Ni–Co–Mn–Sn alloy system is vital for understanding the temperature-dependent composition, practical properties, and physical phenomena in this compound (see Fig. 8). Cong et al. [80] detailed that the magnetic properties and both the temperature and magnetic-field-induced structural transformations in the $Ni_{50-x}Co_xMn_{39}Sn_{11}$ ($0 \le x \le 10$) multifunctional alloys over a large temperature range from 500 K down to 10 K was performed. It's uncovered that, with expanding x, the martensitic transformation temperatures first decrease slowly when $0 \le x \le 4$ and then decrease rapidly when $5 \le x \le 8$; no martensitic transformation was observed in the alloys with $9 \le x \le 10$. The attractive properties of these alloys are very sensitive to their chemical composition. They noted from dependent on the outcomes of attractive and basic advances, the total phase diagram of the $Ni_{50-x}Co_xMn_{39}Sn_{11}$ ($0 \le x \le 10$) alloy system, from high

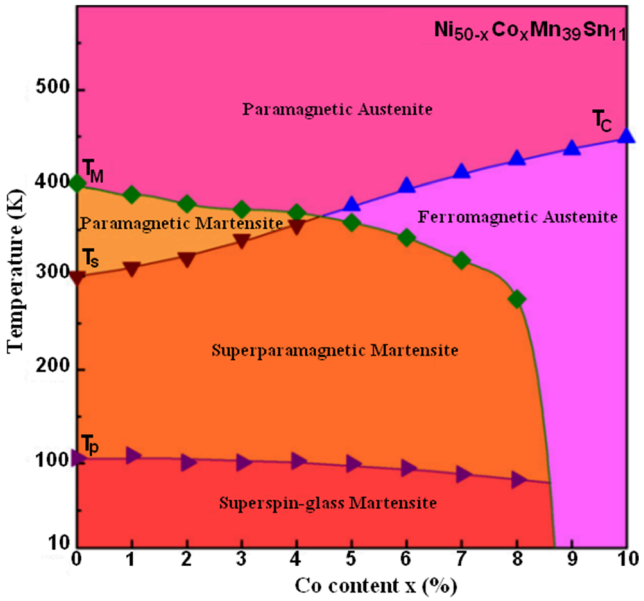

Fig. 8 Phase diagram of the $Ni_{50-x}Co_xMn_{39}Sn_{11}$ ($0 \le x \le 10$) alloy system. Reproduced from reference [79]

temperature down to 10 K, is set up. This phase diagram can be used for the plan of multifunctional alloys with particular properties. Li et al. [81] contemplated the stage progress and magnetocaloric properties of the $Mn_{50}Ni_{42-x}Co_xSn_8$ ($0 \le x \le 10$) alloys. They showed that the martensite has a 6 M monoclinic structure, which the austenite has a $L2_1$ cubic structure. On account of an attractive field change of 5 T, the magnetic entropy change values ΔS_M, for the $Mn_{50}Ni_{36}Co_6Sn_8$, $Mn_{50}Ni_{35}Co_7Sn_8$, and $Mn_{50}Ni_{34}Co_8Sn_8$ ribbons are 14.1, 18.6, and 16.0 J kg^{-1} K^{-1}, respectively. Subsequently, contrasted with the Mn–Ni–Sn ternary alloys, the addition of Co permits a solid magnetostructural coupling over a wide temperature range with enhanced magnetocaloric properties in $Mn_{50}Ni_{42-x}Co_xSn_8$ combinations. Wang et al. [82] revealed that the 2 at% Co-doping to the $Ni_{49}Mn_{39}Sn_{12}$ combination enhances the martensitic transformation temperatures about 25 K; in any case, it does not create any impact on the gem structure of the martensite. They noticed that the distinction in magnetization between martensite and austenite through the martensitic transformation increases strikingly. In this way, the magnetic transition temperature for martensite increments from 320 to 342 K with an expansion of 2 at% Co. Instead of the examinations on the MCE in Ni–Co–Mn–Sn alloys, electrical and thermal transports were scarcely investigated. Chen et al. [83] examined the thermo-control and resistivity regards in zero magnetic fields for $Ni_{47.5}Co_{2.5}Mn_{37}Sn_{13}$ tests. It's found that the electrical transport is metallic, anyway by virtue of the paramagnetic and ferromagnetic austenite stages, a distinction in inclination occurs toward the start of the ferromagnetic change. Chen et al. [84] observed the martensitic transformation in Ti-doped $Ni_{43-x}Ti_xCo_7Mn_{43}Sn_7$. It's confirmed that MT decreases and the mechanical properties are obviously improved by adding an appropriate amount of Ti. The experimental results confirm that the compressive strength and compressive strain of $Ni_{42.5}Ti_{0.5}Co_7Mn_{43}Sn_7$ alloy reach a maximum value of 1760 MPa and 23%, respectively [84]. Although the addition of Ti may improve the ductility to some extent, the substitution of Ti for Ni does not change the brittle nature of NiCoMnSn alloy.

3.3 Characteristics and properties of Ni–Co–Mn–Sb alloys

As effectively noticed, a few investigations have likewise reported the magnetic properties of the Ni–Mn–Sb alloys [62, 63]. In order to create new and better materials having a place with this serie and to test the impact of structural variation on ECM, late examinations have explored the fractional substitution of Co for Ni in the non-stoichiometric Ni–Mn–Sb alloy [85–93]. Nayak et al. [85] reported the effect of Co on the structural, attractive, and magnetocaloric impact of $Ni_{50-x}Co_xMn_{38}Sb_{12}$ alloys with $x = 0$, 2, 3, 4, and 5. They noticed that the martensitic progress temperature is found to diminish monotonically with Co focus. The estimation of the entropy change in $Ni_{45}Co_5Mn_{38}Sb_{12}$ compound is 29 J kg^{-1} K^{-1} at room temperature, while this estimation comes to 34 J kg^{-1} K^{-1} at 262 K under a magnetic field of 5 T. Sahoo et al. [92] analyzed the magnetic properties of as spun ribbon with the annealed ribbon and the bulk alloy of $Ni_{46}Co_4Mn_{38}Sb_{12}$, and observed that MT of as-spun ribbon was higher than that of the bulk sample, while the magnetization of as-spun ribbon was lower. In $Ni_{46}Co_4Mn_{38}Sb_{12-x}Z_x$ (Z = Si, Ga), the Si substitution for Sb balances out the austenite stage, whereas, the Ga substitution stabilizes the martensite phase. With $x = 1$ for Si, the change martensitic abatements to 254 K, and a large MCE of 70 J kg^{-1} K^{-1} are obtained [87]. The content outcomes in reference [86] uncovered the magnetocaloric and magnetotransport properties in Ge-doped Ni–Mn–Sb Heusler compounds. The most extreme ΔS_M estimation of 39 J kg^{-1} K^{-1} was gotten in the warming mode at 273.5 K with a 50 kOe field change, while, a maximum estimation of 42 J kg^{-1} K^{-1} was obtained in cooling mode at 272.5 K in a similar field. Nayak et al. [88] analyzed the effect of weight on the magnetic properties and the magnetocaloric effect in Ni–Co–Mn–Sb Heusler combination.

The temperature dependence of magnetization under various pressures (0–9 kPa) shows that MT moves to higher temperature with the expansion in the pressure, and the martensitic stage is overhauled under pressure, while the isothermal magnetic entropy change decreases with the extension in the pressure. The field dependence of resistivity (ρ(H)) in $Ni_{45}Co_5Mn_{38}Sb_{12}$ at different temperatures represents that the martensitic arrange which changes to parent stage couldn't absolutely recover to its original state without an outer magnetic field. It is attested that the austenite phase would be able

to be stuck and the transformation couldn't be totally reversible in the field dependence of resistivity, and heat capacity [94]. At the point, when rehashed temperature/field cycling is connected in $Ni_{45}Co_5Mn_{38}Sb_{12}$, the resistivity on a very basic level increases and the magnetization decreases due to the microstructural deformation and lattice disorder [88]. Millan-Solsona et al. [95] examined the polycrystalline Ni–Mn–Sb–Co magnetic shape memory alloys which are known to exhibit a magnetocaloric effect. They are accounted that the entropy change values related to the elastocaloric effect. They have demonstrated that uniaxial compressive stresses up to 100 MPa can be connected to the alloys, and the gotten qualities for the entropy change (ΔS = 21 J kg^{-1} K^{-1}) at these stresses compare favorably to ΔS values detailed for non-magnetic shape memory alloys.

In summary, a large portion of the properties of the quaternary Ni–Co–Mn–Y (Y = In, Sn, Sb) Heusler-type $MSMA_s$ outflank those of the Ni–Mn–X (X = In, Sn, Sb) ternary systems.

- The Ni–Co–Mn–In alloy has great metamagnetic properties in which the large magnetization change is ~ 80 A m^2 Kg^{-1} during the martensitic progress. It reveals the largest change in magnetocaloric entropy among quaternary systems.
- The Ni–Co–Mn–Sn compound has a low thermal hysteresis about 10 K and a low magnetic hysteresis about 1.5 T.
- The Ni–Co–Mn–Sb compound demonstrates a high magnetoresistance more noteworthy 70%.

4 Conclusion

This paper is committed to a review of exploratory examinations on phase transitions magnetic and mechanical properties of Heusler Ni–Mn–X (X = In, Sn, Sb) and Ni–Co–Mn–Y (Y = In, Sn, Sb) shape memory alloys. Various studies believe that they have examined the multifunctional properties of these Heusler alloys. These materials have many multifunctional properties, for example, metamagnetic properties: correspondent (ferromagnetic-antiferromagnetic and martensitic advances), shape memory effect, exceptional magnetocaloric impact, and giant magnetoresistance. The idea of high recovery stress, high stress output, high reaction recurrence, and exact control make for an expansive point of view in scientific research and applications design. Be that as it may, the investigation of these alloys has burdens, for example, these alloys with poor mechanical properties normally crack under repeated stress cycles and the cooling life is reduced. The real utilization of magnetocaloric materials and elastocaloric materials requires good mechanical properties. Unfortunately, at present, the main disadvantage of existing $MSMA_s$ is its very fragile nature and poor mechanical properties. Therefore, it's urgent to solve the brittleness problem. In addition, due to the coupling of the martensitic transformation and the ferromagnetic transition, the $MSMA_s$ have a lower operating temperature. However, very few studies have been conducted to increase the operating temperature of these $MSMA_s$, which is also one of the main requirements of the practical applications. The advancement of $MSMA_s$ is even at the research stage and the degree is limited. New applications, for example, in the fields of the actuator and the magnetic sensor must be studied. It is clear that the fundamental research in materials science and Heusler MSMAs applications are still in the beginning.

Funding information This work was funded by the"Taishan Scholar" Project of Shandong Province and Key Basic Research Project of Shandong Natural Science Foundation of China (No. ZR2017ZB0422).

References

1. Perez-Landazabal JI, Recarte V, Sanchez-Alarcos V, Gomez-Polo C, Cesari E (2013) Magnetic properties of the martensitic phase in Ni-Mn-In-Co metamagnetic shape memory alloys. J Appl Phys Lett 102:101908
2. Kainuma R, Imano Y, Ito W, Sutou Y, Morito H, Okamoto S, Kitakami O, Oikawa K, Fujita A, Kanomata T, Ishida K (2006) Magnetic-field-induced shape recovery by reverse phase transformation. Nature 439:957–960
3. Yu SY, Cao ZX, Ma L, Liu GD, Chen JL, Wu GH, Zhang B, Zhang XX (2007) Realization of magnetic field-induced reversible martensitic transformation in NiCoMnGa alloys. J Appl Phys Lett 91: 102507
4. Liu ZH, Liu H, Zhang XX, Zhang XK, Xiao JQ, Zhu ZY, Dai XF, Liu GD, Chen JL, Wu GH (2005) Large negative magnetoresistance in quaternary Heusler alloy $Ni_{50}Mn_8Fe_{17}Ga_{25}$ melt-spun ribbons. J Appl Phys Lett 86:182507
5. Liu J, Gottschall T, Skokov KP, Moore JD, Gutfleisch O (2012) Giant magnetocaloric effect driven by structural transitions. Nat Mater 11:620–626
6. Du J, Zheng Q, Ren WJ, Feng WJ, Liu XG, Zhang ZD (2007) Magnetocaloric effect and magnetic-field-induced shape recovery effect at room temperature in ferromagnetic Heusler alloy Ni-Mn-Sb. J Phys D Appl Phys 40:5523–5526
7. Marioni MA, O'Handley ROC, Allen SM, Hall SR, Paul DJ, Richard ML (2005) The ferromagnetic shape memory effect in Ni-Mn-Ga. J Magn Magn Mater 290:35
8. Brown GV (1976) Magnetic heat pumping near room temperature. J Appl Phys 47:3673–3680
9. Pecharsky VK, Gschneider KA (2006) Magnetic refrigeration. Int J Refrig 29:1239–1249
10. Otsuka K, Ren X (2005) Physical metallurgy of Ti–Ni-based shape memory alloys. Prog Mater Sci 50:511–678
11. Oliveira JP, Miranda RM, Braz Fernandes FM (2017) Welding and joining of NiTi shape memory alloys: a review. Prog Mater Sci 88: 412–466. https://doi.org/10.1016/j.pmatsci.2017.04.008
12. Smart materials and structures. By M. V. Gandhi and B. S. Thompson, Chapman and Hall, London 1992, 310 pp., hardback, ISBN 0-412-37010-7. Adv Mater, 5: 313-314. https://doi.org/10.1002/adma.19930050427

13. Heusler F, Stark W, Haupt E (1903) Über magnetische manganlegierungen. Verhandlungen der Deutschen Physikalischen Gesellschaft 5
14. Heusler F, Richarz F (1909) Studien über magnetisierbare manganlegierungen. Z Anorg Chem 61:265–279
15. Bradley AJ, Rodgers JW (1934) The crystal structure of the Heusler alloys. Proceedigs of the Royal Society of London. Series A, Containing Papers of a Mathematical and Physical Character 50: 2024–2027.https://doi.org/10.1098/rspa.1934.0053
16. Groot RA, Mueller FM, PGV E, Buschow KHJ (1983) New class of materials: half-metallic ferromagnets. Phys Rev Lett 50:2024–2027
17. Graf T, Felser C, Parkin SSP (2011) Simple rules for the understanding of Heusler compounds. Prog Solid State Chem 39:1–50
18. Wang CW, Wang JM, Jiang CB (2013) A linear elastic $Ni_{50}Mn_{25}Ga_9Cu_{16}$ martensitic alloy. Rare Metals 32:29–32
19. Trudel S, Gaier O, Hamrle J, Hillebrands B (2010) Magnetic anisotropy, exchange and damping in cobalt-based full-Heusler compounds: an experimental review. J Phys D Appl Phys 43:193001
20. Kreiner G, Kalache A, Hausdorf S, Alijani V, Qian JF, Shan G, Burkhardt U, Ouardi S, Felser C (2014) New Mn_2-based Heusler compounds. Z Anorg Allg Chem 640:738–752
21. Louidi S, Suñol JJ, Bachaga T, González-Legarreta L, Rosa WO, Hernando B (2014) Thermomagnetic and structural analysis of as-quenched Ni49Co1Mn37Sn13. Phys Status Solidi C 11:1116–1119. https://doi.org/10.1002/pssc.201300700
22. Liu G, Dai X, Liu H, Chen J, Li Y, Xiao G, Wu G (2008) Mn_2CoZ (Z = Al, Ga, In, Si, Ge, Sn, Sb) compounds: structural, electronic, and magnetic properties. Phys Rev B 77:014424
23. Dikshtein I, Koledov V, Shavrov V, Tulaikova A, Cherechukin A, Buchelnikov V, Khovailo V, Matsumoto M, Takagi T, Tani J (1999) Phase transitions in intermetallic compounds Ni-Mn-Ga with shape memory effect. IEEE Trans Magn 35:3811–3813
24. Dai XF, Wang HY, Chen LJ, Duan XF, Chen JL, Wu GH, Zhu H, Xiao JQ (2006) Growth and characterization of ferromagnetic shape memory alloy $Co_{50}Ni_{20}FeGa_{29}$ single crystals. J Cryst Growth 290:626–630
25. Peterson BW, Allen SM, O'Handley RC (2008) Temperature dependence of the magnetic-field-induced strain of NiMnGa in the presence of an acoustic drive. J Appl Phys 104:033918
26. Bachaga T, Daly R, Khitouni M, Escoda L, Saurina J, Suñol JJ (2015) Thermal and structural analysis of $Mn_{49.3}Ni_{43.7}Sn_{7.0}$ Heusler Alloy Ribbons. Entropy 17:646–657
27. Liu J, Scheerbaum N, Hinz D, Gutfleisch O (2008) Magnetostructural transformation in Ni-Mn-In-Co ribbons. J Appl Phys Lett 92:162509
28. Rekik H, Chemingui M, Bachaga T, Cherif A, Bruna P, Sunol JJ and Khitouni M (2015) Structure and Mössbauer analysis of melt-spun Fe-Pd ribbons containing Ni and Co. Metals, 1020-1028. https://doi.org/10.3390/met5021020
29. Pons J, Segui C, Chernenko VA, Cesari E, Ochin P, Portier R (1999) Transformation and ageing behaviour of melt-spun Ni-Mn-Ga shape memory alloys. Mater Sci Eng A 273:315–319
30. Ullakko K, Huang JK, Kantner C, O'Handley RC, Kokorin VV (1996) Large magnetic-field-induced strains in Ni_2MnGa single crystals. J Appl Phys Lett 69:1966–1968
31. Ranjan R, Banik S, Barman SR, Kumar U, Mukhopadhyay PK, Pandey D (2006) Powder x-ray diffraction study of the thermoelastic martensitic transition in Ni2Mn1.05Ga0.95. Phys Rev B 74:224443
32. Dikshtein I, Koledov V, Shavrov V, Tulaikova A, Cherechukin A (1999) Phase transitions in intermetallic compounds Ni-Mn-Ga with shape memory effect. IEEE Trans Magn 35:3811–3813
33. Acet M, Mañosa L, Planes A (2011) Magnetic-field-induced effects in martensitic Heusler-based magnetic shape memory alloys. K. H. J. Buschow (Ed.). Handb Magn Mater 19:231
34. Khovaylo VV, Buchelnikov VD, Kainuma R, Koledov VV, Ohtsuka M, Shavrov VG, Takagi T, Taskaev SV, Vasiliev AN (2005) Phase transitions in $Ni_{2+x}Mn_{1+x}Ga$ with a high Ni excess. Phys Rev B 72:224408
35. Aksoy S, Krenke T, Acet M, Wassermann EF, Moya X, Mañosa L, Planes A (2007) Magnetization easy axis in martensitic Heusler alloys estimated by strain measurements under magnetic field. J Appl Phys Lett 91:251915
36. Planes A, Mañosa L, Acet M (2009) Magnetocaloric effect and its relation to shape-memory properties in ferromagnetic Heusler alloys. J Phys Condens Matter 21:233201
37. Krenke T, Acet M, Wassermann E, Moya X, Manosa L, Planes A (2005) Martensitic transitions and the nature of ferromagnetism in the austenitic and martensitic states of Ni-Mn-Sn alloys. Phys Rev B 72:014412
38. Krenke T, Acet M, Wassermann E, Moya X, Manosa L, Planes A (2006) Ferromagnetism in the austenitic and martensitic states of Ni-Mn-In alloys. Phys Rev B 73:174413
39. Wang HF, Wang JM, Jiang CB, Xu HB (2014) Phase transition and mechanical properties of $Ni_{30}Cu_{20}Mn_{37+x}Ga_{13-x}$(x = 0–4.5) alloys. Rare Metals 33:547–551
40. Li Z, Jing C, Zhang HL, Qiao YF, Cao SX, Zhang JC, Sun L (2009) A considerable metamagnetic shape memory effect without any prestrain in $Ni_{46}Cu_4Mn_{38}Sn_{12}$ Heusler alloy. J Appl Phys 106: 083908
41. Takenaga T, Hayashi K, Kajitani T (2007) Structural and magnetic transition temperatures of full Heusler Ni-Mn-Sn alloys determined by Van der Pauw method. J Chem Eng Jpn 40:1328–1329
42. Hernando B, Sánchez Llamazares JL, Santos JD, Sánchez ML, Ll E, Suñol JJ, Varga R, García C, González J (2009) Grain oriented NiMnSn and NiMnIn Heusler alloys ribbons produced by melt spinning: martensitic transformation and magnetic properties. J Magn Magn Mater 321:763–768
43. Bachaga T, Rekik H, Krifa M, Sunol JJ, Khitouni M (2016) Investigation of the enthalpy/entropy variation and structure of Ni–Mn–Sn(Co, In) melt-spun alloys. J Therm Anal Calorim https://doi.org/10.1007/s10973-016-5716-z
44. Coll R, Saurina J, Escoda L, Sunol JJ (2018) Thermal analysis of $Mn_{50}Ni_{50-x}(Sn, In)_x$ Heusler shape memory alloys. J Therm Anal Calorim 134:1277–1284. https://doi.org/10.1007/s10973-018-7551-x
45. Bachaga T, Daly R, Escoda L, Sunol JJ, Khitouni M (2015) Influence of chemical composition on martensitic transformation of MnNiIn shape memory alloys. J Therm Anal Calorim 122: 167–173
46. Barandiaran JM, Chernenko VA, Cesari E, Salas D, Lazpita P, Gutierrez J, Orue I (2013) Magnetic influence on the martensitic transformation entropy in Ni-Mn-In metamagnetic alloy. J Appl Phys Lett 102:071904
47. González-Legarreta L, González-Alonso D, Rosa WO, Caballero-Flores R, Suñol JJ, González J, Hernando B (2015) Magnetostructural phase transition in off-stoichiometric Ni-Mn-In Heusler alloy ribbons with low In content. J Magn Magn Mater 383:190–195
48. Sutou Y, Imano Y, Koeda N, Omori T, Kainuma R, Ishida K, Oikawa K (2004) Magnetic and martensitic transformations of NiMnX (X = In, Sn, Sb) ferromagnetic shape memory alloys. J Appl Phys Lett 85:4358
49. Yiwen J, Li Z, Li Z, Yang Y, Yang B, Zhang Y, Esling C, Zhao X, Zuo L (2017) Magnetostructural transformation and magnetocaloric effect in Mn-Ni-Sn melt-spun ribbons. Eur Phys J Plus 132:1. https://doi.org/10.1140/epjp/i2017-11316-1
50. Khan M, Dubenko I, Stadler S, Ali N (2008) Magnetostructural phase transitions in $Ni_{50}Mn_{25+x}Sb_{25-x}$ Heusler alloys. J Phys Condens Matter 20:235204

51. Santos JD, Sánchez T, Álvarez P, Sánchez ML, Sánchez ML, Sánchez Llamazares JL, Hernando B (2008) Microstructure and magnetic properties of Ni50Mn37Sn13 Heusler alloy ribbons. J Appl Phys Lett 103:07B326
52. Muthu S, Rama Rao NV, Maniel Raja M, Raj Kumar DM, Mohan Radheep D, Arumugan S (2010) Influence of Ni/Mn concentration on the structural, magnetic and magnetocaloric properties in $Ni_{50-x}Mn_{37+x}Sn_{13}$ Heusler alloys. J Phys D Appl Phys 43:425002
53. Krenke T, Duman E, Acet M, Wassermann EF, Moya X, Mañosa L, Planes A (2005) Inverse magnetocaloric effect in ferromagnetic Ni-Mn-Sn alloys. Nat Mater 4:450–454
54. Ghosh A, Mandal K (2013) Large magnetic entropy change and magnetoresistance associated with a martensitic transition of Mn-rich Mn50.5−xNi41Sn8.5+x alloys. J Phys D Appl Phys 46: 435001
55. Caballero-Flores R, González-Legarreta L, Rosa WO, Sánchez T, Prida VM, Escoda L, Suñol JJ, Btdalovd AB, Alievd AM, Koledove VV, Shavrove VG, Hernando B (2015) Magnetocaloric effect, magnetostructural and magnetic phase transformations in Ni50.3Mn36.5Sn13.2 Heusler alloy ribbons. J Alloys Compds 629:332–342
56. Ray MK, Bagani K, Banerjee S (2014) Effect of excess Ni on martensitic transition, exchange bias and inverse magnetocaloric effect in $Ni_{2+x}Mn_{1.4-x}Sn_{0.6}$ alloy. J Alloys Compds 600:55–59
57. Aydogdu Y, Turabi AS, Kok M, Aydogdu A, Yakinci ZD, Aksan MA, Yakinci ME, Karaca HE (2016) The effect of Sn content on mechanical, magnetization and shape memory behavior in NiMnSn alloys. J Alloys Compd 683:339–345
58. Tan CL, Feng ZC, Zhang K, Wu MY, Tian XH, Guo EJ (2017) Microstructure, martensitic transformation and mechanical properties of Ni-Mn-Sn alloys by substituting Fe for Ni. Trans Nonferrous Metals Soc China 27:2234–2223
59. Stern-Taulats E, Castillo-Villa PO, Manosa L, Frontera C, Pramanick S, Majumdar S, Planes A (2014) Magnetocaloric effect in the low hysteresis Ni-Mn-In metamagnetic shape-memory Heusler alloy. J Appl Phys 115:173907
60. Rosa WO, Gonzalez L, Garcıa J, Sanchez T, Vega V, Escoda L, Sunol JJ, Santos JD, Alves MJP, Sommer RL, Prida VM, Hernando B (2012) Tailoring of magnetocaloric effect in $Ni_{45.5}Mn_{43.0}In_{11.5}$ metamagnetic shape memory alloy. Phys Res Inter 5. https://doi.org/10.1155/2012/794171
61. Huang YJ, Hu QD, Bruno NM, Chen J-H, Karaman I, Ross Jr JH, Li JG (2015) Giant elastocaloric effect in directionally solidified Ni-Mn-In magnetic shape memory alloy. Scr Mater 105:42–45
62. Khan M, Ali N, Stadler S (2007) Inverse magnetocaloric effect in ferromagnetic $Ni_{50}Mn_{(37+x)}Sb_{(13-x)}$ Heusler alloys. J Appl Phys 101:053919
63. Feng WJ, Zhang Q, Zhang LQ, Li B, Du J, Deng YF, Zhang ZD (2010) Large reversible high-temperature magnetocaloric effect in $Ni_{50-x}Mn_{38+x}Sb_{12}$ alloys. Solid State Commun 150:949–952
64. Liu J, Gottschall T, Skokov KP, Moore JD, Gutfleisch O (2012) Giant magnetocaloric effect driven by structural transitions. Nat Mater 11:620–626
65. Huang L, Cong DY, Ma L, Nie ZH, Wang ZL, Suo HL, Ren Y, Wang YD (2016) Large reversible magnetocaloric effect in a Ni-Co-Mn-In magnetic shape memory alloy. Appl Phys Lett 108: 032405
66. Monroe JA, Karaman I, Basaran B, Ito W, Umetsu RY, Kainuma R, Koyama K, Chumlyakov YI (2012) Direct measurement of large reversible magnetic-field-induced strain in Ni-Co-Mn-In metamagnetic shape memory alloys. Acta Mater 60:6883–6891
67. Xu X, Kihara T, Tokunaga M, Matsuo A, Ito W, Umetsu RY, Kindo K, Kainuma R (2013) Magnetic field hysteresis under various sweeping rates for Ni-Co-Mn-In metamagnetic shape memory alloys. J Appl Phys Lett 103:122406
68. Li Z, Li Z, Yang B, Zhao X, Zuo L (2018) Giant low-field magnetocaloric effect in a textured Ni45.3Co5.1Mn36.1In13.5 alloy. Script Mater 151:61–65
69. Emre B, Yuce S, Stern-Taulats E, Planes A, Fabbrici S, Albertini F, Manosa L (2013) Large reversible entropy change at the inverse magnetocaloric effect in Ni-Co-Mn-Ga-In magnetic shape memory alloys. J Appl Phys 113:213905
70. Kihara T, Xu X, Ito W, Kainuma R, Tokunaga M (2014) Direct measurements of inverse magnetocaloric effects in metamagnetic shape-memory alloy NiCoMnIn. Phys Rev B 90:214409
71. Manosa L, González-Alonso D, Planes A, Bonnot E, Barrio M, Tamarit JL, Aksoy S, Acet M (2010) Giant solid-state barocaloric effect in the Ni-Mn-In magnetic shape-memory alloy. Nat Mater 9: 478–481
72. De Oliveira N (2007) Entropy change upon magnetic field and pressure variations. J Appl Phys Lett 90:052501
73. Sakon T, Yamazaki S, Kodama Y, Motokawa M, Kanomata T, Oikawa K, Kainuma R, Ishida K (2007) Magnetic Field-Induced Strain of Ni–Co–Mn–In Alloy in Pulsed Magnetic Field. Jpn J Appl Phys 46:995–998
74. Liu HS, Zhang CL, Han ZD, Xuan HC, Wang DH, Du YW (2009) The effect of Co doping on the magnetic entropy changes in $Ni_{44-x}Co_xMn_{45}Sn_{11}$ alloys. J Alloys Compd 467:27–30
75. Feng Y, Chen H, Xiao F, Bian X, Wang P (2018) Improvement of mechanical property and large shape recovery of sintered $Ni_{45}Mn_{36.6}In_{13.4}Co_5$ alloy. J Alloy Compds 765:264–270
76. Bachaga T, Daly R, Suñol JJ, Saurina J, Escoda L, Legarreta L, Hernando B, Khitouni M (2015) Effects of Co additions on the martensitic transformation and magnetic properties of Ni-Mn-Sn shape memory alloys. J Supercond Nov Magn 28:3087–3092
77. Jing C, Li Z, Zhang HL, Chen JP, Qiao YF, Cao SX, Zhang JC (2009) Martensitic transition and inverse magnetocaloric effect in Co doping Ni-Mn-Sn Heusler alloy. Eur Phys J B 67:193–196
78. Deltell A, Escoda L, Saurina J, Suñol JJ (2015) Martensitic transformation in Ni-Mn-Sn-Co Heusler alloys. Metals 5:695–705
79. Cong DY, Roth S, Potschke M, Hurrich C, Schultz L (2010) Phase diagram and composition optimization for magnetic shape memory effect in Ni-Co-Mn-Sn alloys. J Appl Phys Lett 97:021908
80. Cong DY, Roth S, Schultz L (2012) Magnetic properties and structural transformations in Ni-Co-Mn-Sn multifunctional alloys. Acta Mater 60:5335–5351
81. Li Z, Jiang Y, Li Z, Sánchez Valdés CF, Sánchez Llamazares JL, Yang B, Zhang Y, Esling C, Zhao X, Zuo L (2018) Phase transition and magnetocaloric properties of $Mn_{50}Ni_{42-x}Co_xSn_8$ ($0 \le x \le 10$) melt-spun ribbons. IUCrJ 5:54
82. Wang W, Yu J, Zhai Q, Luo Z, Zheng H (2013) Co-doping effect on the martensitic transformation and magnetic properties of $Ni_{49}Mn_{39}Sn_{12}$ alloy. J Magn Magn Mater 346:103–106
83. Chen X, Naik VB, Mahendiran R, Ramanujan RV (2015) Optimization of Ni-Co-Mn-Sn Heusler alloy composition for near room temperature magnetic cooling. J Alloys Compd 618:187–191
84. Chen F, Tong YX, Tian B, Li L, Zheng YF (2014) Martensitic transformation and magnetic properties of Ti-doped NiCoMnSn shape memory alloy. Rare Metals 33:511–515
85. Nayak AK, Suresh KG, Nigam AK (2009) Observation of enhanced exchange bias behaviour in Ni-Co-Mn-Sb Heusler alloys. J Phys D Appl Phys 42:115004
86. Nayak AK, Suresh KG, Nigam AK (2010) Magnetic, electrical and magneto thermal properties in NiCoMnSb Heusler alloys. J Appl Phys 107:09A927
87. Nayak AK, Suresh KG, Nigam AK (2011) Correlation between reentrant spin glass behavior and the magnetic order–disorder transition of the martensite phase in Ni-Co-Mn-Sb Heusler alloys. J Phys Condens Matter 23:416004
88. Nayak AK, Suresh KG, Nigam AK (2011) Anomalous effects of repeated martensitic transitions on the transport, magnetic and

thermal properties in Ni-Co-Mn-Sb Heusler alloy. Acta Mater 59: 3304–3312
89. Nayak AK, Suresh KG, Nigam AK (2011) Metastability of magneto-structural transition revealed by sweep rate dependence of magnetization in Ni45Co5Mn38Sb12 Heusler alloy. J Appl Phys 109:07A906
90. Nayak AK, Suresh KG, Nigam AK (2009) Giant inverse magnetocaloric effect near room temperature in Co substituted NiMnSb Heusler alloys. J Phys D Appl Phys 42:035009
91. Sahoo R, Raj Kumar DM, Arvindha Babu D, Suresh K, Nigam G, Manivel AK, Raja M (2013) Effect of annealing on the magnetic, magnetocaloric and magnetoresistance properties of Ni-Co-Mn-Sb melt spun ribbons. J Magn Magn Mater 347:95–100
92. Sahoo R, Nayak AK, Suresh KG, Nigam AK (2011) Effect of Si and Ga substitutions on the magnetocaloric properties of NiCoMnSb quaternary Heusler alloys. J Appl Phys 109:07A921
93. Nayak AK, Suresh KG, Nigam AK, Coelho AA, Gama S (2009) Pressure induced magnetic and magnetocaloric properties in NiCoMnSb Heusler alloy. J Appl Phys 106:053901
94. Nayak AK, Suresh KG, Nigam AK (2010) Irreversibility of field induced magnetostructural transition in NiCoMnSb shape memory alloy revealed by magnetization, transport and heat capacity studies. J Appl Phys Lett 96:112503
95. Millan-Solsona R, Stern-Taulats E, Vives E, Planes A, Sharma J, Nayak AK, Suresh KG, Manosa L (2014) Large entropy change associated with the elastocaloric effect in polycrystalline Ni-Mn-Sb-Co magnetic shape memory alloys. J App Phys Lett 105:24190